The Fifth International Symposium on Computational Wind Engineering (CWE2010)
Chapel Hill, North Carolina, USA May 23-27, 2010

Numerical study on steady aerodynamic characteristics of ice accreted transmission lines

Shinichi Oka[a], Takeshi Ishihara[b]

[a]*NUMECA Japan Co,. Ltd., AIOS Bldg. 2-15-19, Kamiosaki, Shinagawa-ku, Tokyo 141-0021, Japan*
[b] *Department of Civil Engineering, School of Engineering, The University of Tokyo, 7-3-1 Hongo, Bunkyo-ku, Tokyo 113-8656, Japan*

ABSTRACT: Aerodynamic characteristics of ice accreted transmission line has been investigated using LES turbulence model. The results show that predicted mean aerodynamic coefficients for single and 4-conductor bundle favorably agree with wind tunnel test results including acute change of lift coefficients. Mechanism of peak lift coefficients was verified by investigating pressure field for comprehensive understanding of the phenomenon. A method of obtaining mean aerodynamic coefficients of 4-conductor bundle converted from those of single conductor is proposed, and verified by the numerical analysis.

1 INTRODUCTION

The large amplitude wind-induced motion of ice accreted transmission lines, called galloping, could cause inter-phase short circuit, damage of insulators and support structures, and, in the worst case, resulting shutdown of transmission lines. Hence, it is important to understand and predict the galloping phenomenon to establish counter measure to prevent an accident. Many studies have performed to assess the galloping phenomenon (Den Hartog, 1956; Parkinson, 1971; Novak, 1972; Cooper, 1973; Kimura, et al., 1999; Inoue, 2000; Shimizu et al., 2004; Phuc et al., 2005). Shimizu developed the finite element analysis code that requires mean aerodynamic coefficients as input data. Those aerodynamic coefficients data are based on a database in which mean aerodynamic coefficients are interpolated using the past wind tunnel tests results (Shimizu and Sato, 2001).

Aerodynamic coefficients obtained from the wind tunnel test were small in variety for the multi-bundle conductor, and interpolations are used to supplement insufficient data (Shimizu et al., 2004). However, accuracy of interpolated aerodynamic coefficients for various kinds of ice accreted transmission lines is not clear. Recently, Oka and Ishihara (2009) successfully predicted mean and fluctuating aerodynamic coefficients of square prism with various angles of attack. It was noted that spanwise length 1D is practically enough for predicting mean values. This implies that the numerical simulation with LES turbulence model can be alternative method to accurately predict aerodynamic coefficients of bluff body.

As reported by Shimizu et al. (2004), profiles of accreted ice significantly affect aerodynamic coefficients and could cause large negative gradient of lift coefficient, resulting in galloping of ice accreted transmission lines. The mechanism of peaks lift coefficient has not made clear. Shimizu et al. (2004) also proposed a formula to estimate aerodynamic coefficients of 4-conductor bundle by using those of single conductor, however, the result showed inconsistent with experiment at angles of attack where wake from upstream conductors affected the downstream ones.

In this study, aerodynamic characteristics of ice accreted transmission line is investigated by LES turbulence model and compared with the measurements from the wind tunnel test. Section 2 describes the numerical model used in this study. Section 3 presents the predicted aerodynamic coefficients of single conductor from the numerical simulation, which are compared with the experimental data and the interpolated those for the cases of H=0.5*D* and 0.25*D*. The mechanism of peak lift coefficient is also investigated by the pressure distribution of the ice accreted conductor. Finally, a formula considering the velocity reduction in the wake region is proposed to estimate aerodynamic coefficients of 4-conductor bundle by using those of single conductor and compared with the experiment.

2 NUMERICAL MODEL

2.1 *Governing equations*

The governing equations employed in LES model are obtained by filtering the time-dependent Navier-Stokes equations as follows;

$$\frac{\partial \rho \tilde{u}_i}{\partial x_i} = 0 , \tag{1}$$

$$\frac{\partial}{\partial t}(\rho \tilde{u}_i) + \frac{\partial}{\partial x_j}(\rho \tilde{u}_i \tilde{u}_j) = \frac{\partial}{\partial x_j}\left(\mu \frac{\partial \tilde{u}_i}{\partial x_j} \right) - \frac{\partial \tilde{P}}{\partial x_i} - \frac{\partial \tau_{ij}}{\partial x_j}, \tag{2}$$

where $\tilde{u}_j$ and $\tilde{p}$ are filtered mean velocity and filtered pressure respectively. ρ is density and τ_{ij} is subgrid-scale stress. The subgrid-scale stresses resulting from the filtering operations are unknown, and modeled as follows;

$$\tau_{ij} = -2\mu_t \tilde{S}_{ij} + \frac{1}{3}\tau_{kk}\delta_{ij} , \quad \tilde{S}_{ij} \equiv \frac{1}{2}\left(\frac{\partial \tilde{u}_i}{\partial x_j} + \frac{\partial \tilde{u}_j}{\partial x_i} \right), \tag{3}$$

where μ_t is subgrid-scale turbulent viscosity, and $\tilde{S}_{ij}$ is the rate-of-strain tensor.

2.2 *Smagorinsky model*

Smagorinsky model (Smagorinsky, 1963) is used for the subgrid-scale turbulent viscosity.

$$\mu_t = \rho L_s^2 \left| \tilde{S} \right| = \rho L_s \sqrt{2\tilde{S}_{ij}\tilde{S}_{ij}} , \tag{4}$$

where L_s is the mixing length for subgrid-scales, and defined as;

$$L_s = \min\left(\kappa\delta, C_s V^{1/3} \right). \tag{5}$$

where κ is the von Karman constant, 0.42, C_s is Smagorinsky constant, 0.032 , δ is the distance to the closest wall, and V is the volume of a computational cell.

2.3 *Boundary conditions*

When a wall-adjacent cell is in the laminar sublayer, the wall shear stress is obtained from the laminar stress-strain relationship. If the mesh cannot resolve the laminar sublayer, it is assumed that the centroid of the wall-adjacent cells falls within the logarithmic region of the boundary layer, and the law-of-the-wall is employed.

$$\frac{\tilde{u}}{u_\tau}=\frac{\rho u_\tau y}{\mu},\quad \frac{\tilde{u}}{u\tau_\tau}=\frac{1}{\kappa}\ln E\left(\frac{\rho u_\tau y}{\mu}\right) \tag{6}$$

where $\tilde{u}$ is filtered velocity that is tangential to the wall, u_τ is friction velocity, κ is von Kármán constant, and constant E is 9.8. Uniform velocity condition is specified at inlet boundary, and zero diffusive conditions are used at the outlet boundary. Symmetry conditions are given for both sides and upper/lower boundaries.

2.4 *Numerical method*

Finite volume method and unstructured collocated mesh are used for the present simulations. The second order central difference scheme is used for the convective and viscosity term, and the second order implicit scheme for the unsteady term. SIMPLE (Semi-Implicit Pressure Linked Equations) algorithm is employed for solving the discritized equations (Ferziger and Peric, 2002).

2.5 *Modeling conditions and system configurations*

The models of ice accreted transmission line in the present study are based on the wind tunnel test by Shimizu (Shimizu et al., 2004). Figure 1 shows the section of profile of ice accreted single conductor transmission line models in which the heights of accreted ice, H, are respectively,1*D*, 0.5*D*, and 0.25*D*, where *D* denotes diameter of the conductor. Figure 2 shows the computational domain for the single conductor and mesh used in the present study. The computational domain is square as shown in Figure2(a), and length of each side of the domain is 60*D*. Mesh density is higher at the tip of accreted ice and total 288 grids are distributed in the circumference as shown in Figure2(b). Figure 3(a) shows 4-conductor bundle model in which typical diameter *B*, interval between conductor centers, is 13*D*. Mesh distribution in the vicinity of each accreted ice and conductor is the same as that of single conductor transmission line model. As shown in Figure 3(b), structured uniform size grids are distributed between conductors to minimize numerical viscosity. Table 1. shows the conditions of the simulations.

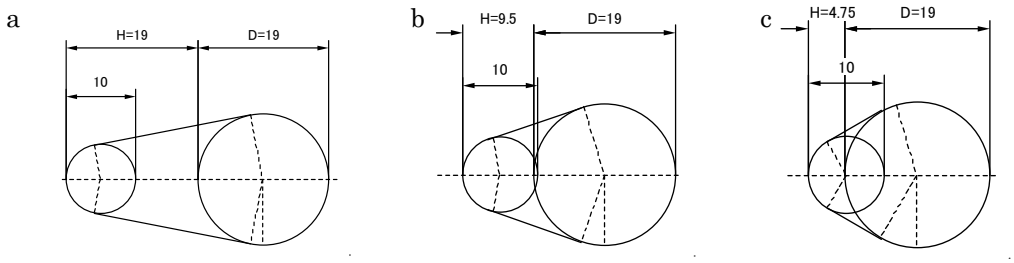

Figure 1. Cross sectional dimensions of conductors and accreted ice model geometry: (a) height of accreted ice H=1D; (b) H=0.5D; (c) H=0.25D

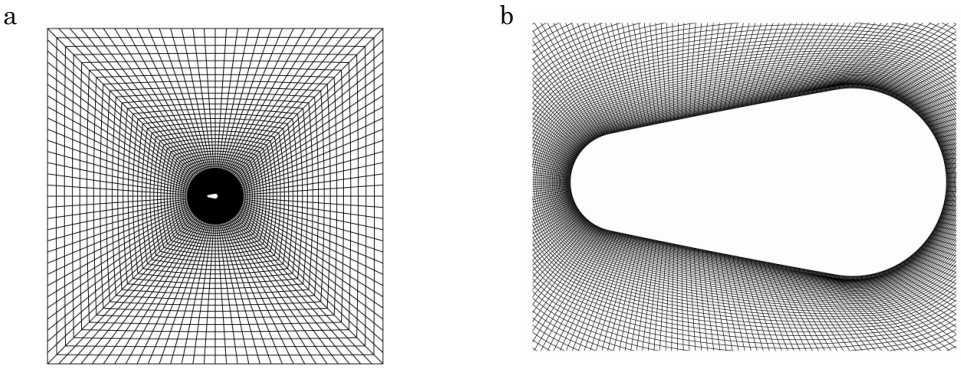

Figure 2. Computational domain and mesh: (a) computational domain of single conductor; (b) mesh near the ice accreted single conductor

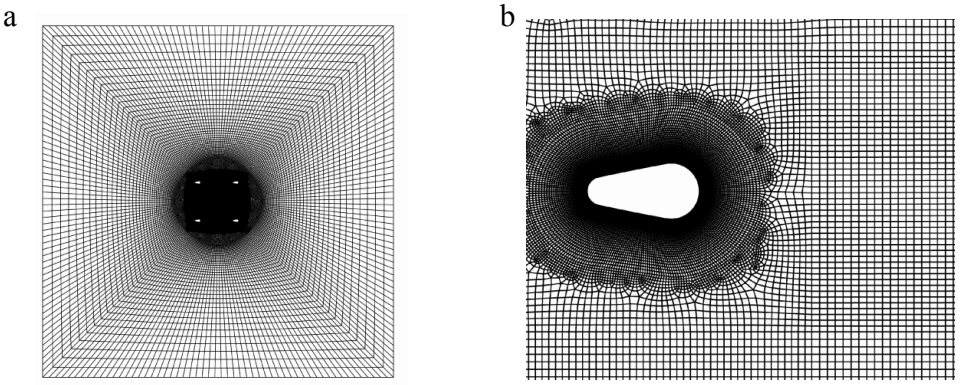

Figure 3. Computational domain and mesh: (a) computational domain of 4-conductor bundle; (b) mesh between ice accreted conductors of 4-conductor bundle

Table 1. Parameter used in this study

Conductor type	Single conductor			4-conductor bundle
Height of accreted ice H	$1D$	$0.5D$	$0.25D$	$1D$
Reynolds number UD/ν			13,000	
Non-dimensional time step size tU/D			0.04	
Spanwise length L		$2D$		$1D$
The number of mesh in spanwise direction N		20		4
The number of the mesh		228,000		349,500

3 MEAN AERODYNAMICS FOR SINGLE CONDUCTOR

Negative gradient of mean lift coefficients could cause negative damping resulting in galloping (Den Hartog, 1956; Parkinson, 1971). Hence, it is important to predict peak of mean lift coefficients. In this section, mean aerodynamic coefficients of single conductor transmission line are predicted for the height of accreted ice, H=1D, 0.5D, and 0.25D, and compared with the wind tunnel test results.

Figure 4 shows mean aerodynamic coefficients, C_D, C_L, C_M, vary with angles of attack in different heights of accreted ice plotted with Shimizu (Shimizu et al., 2004). As shown in Figure 4(a), predicted C_D for H=1D show a flat curve in the range from $\alpha = 0°$ to

12°, then linearly increases with increase in α, which is in good agreement with the experiments. Predicted C_L for H=1D shows negative gradient between $\alpha = 0°$ and 12° as observed in experiment as shown in Figure 4(b). The acute change of C_L around $\alpha = 12°$ as observed in the experiment is well captured by the present numerical approach. Predicted C_L is underestimated the experiment between $\alpha = 12°$ and 30°. In the range from $\alpha = 30°$ or larger, the predicted C_L curve is almost flat and in good agreement with experiment. As shown in Figure 4(b), predicted C_M agrees with experiment for all angles of attack.

Regarding the relation between the height of accreted ice and aerodynamic coefficients, as shown in Figure 4(b), angle of attack at peak lift coefficient, $\alpha = 12°$ for H=1D, is shifted to 20° at H=0.5D, and the magnitude of the peak becomes smaller. The peak is almost disappear at H=0.25D. The angle of attack corresponding to the peaks increase when the height of accreted ice reduces. Similar tendency is observed in the predicted moment coefficients as shown in Figure 4(b). Those predicted results are in good agreement with experiments. Table 2 present mean lift coefficients obtained by interpolations at $\alpha = 20°$ vary with the height of accreted ice at H=0, 0.25D, 0.5D, and 1.0D respectively. As shown in the table, significant discrepancies are observed between C_L by interpolations and experiment for both H=0.25D and 0.5D, and present numerical analysis has advantage over conventional interpolations.

Negative gradient of lift coefficients and peak lift coefficients are observed in the experiment (Shimizu et. al, 2004). However, the mechanism of the phenomenon is not discussed in the study because pressure field data are not available. One of the advantages of the numerical analysis is that comprehensive flow and pressure fields can be obtained from an analysis result.

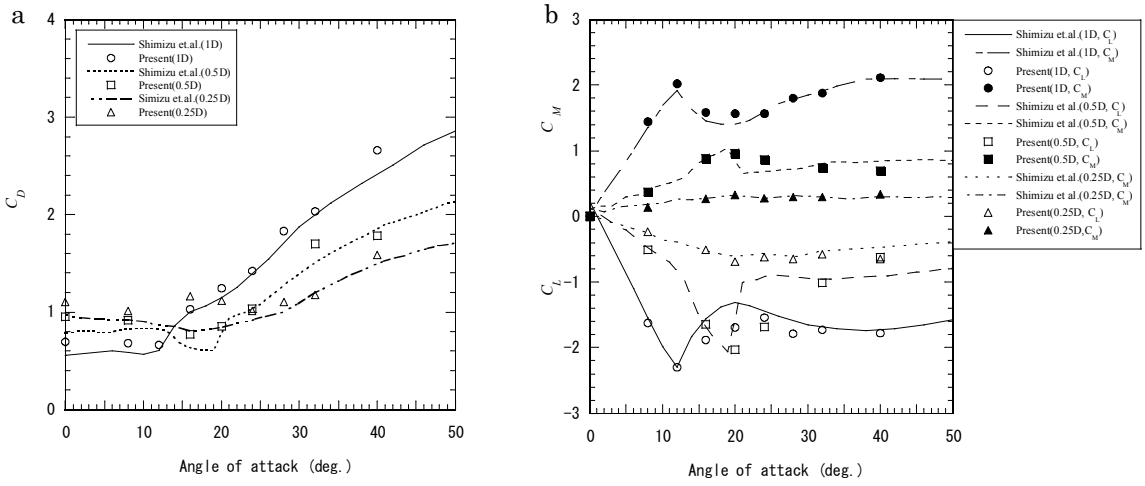

Figure 4. Variations of aerodynamic coefficients with angles of attack : (a) C_D , (b) C_L and C_M for single conductor at H=1D, 0.5D, and 0.25D

Table 2. Mean aerodynamic coefficients obtained by interpolations at α =20°

H	C_L		
	experiment	numerical	interpolation
0	0	0	-
0.25D	-0.61	-0.69	-1.03
0.5D	-2.06	-2.03	-0.66
1.0D	-1.31	-1.70	-

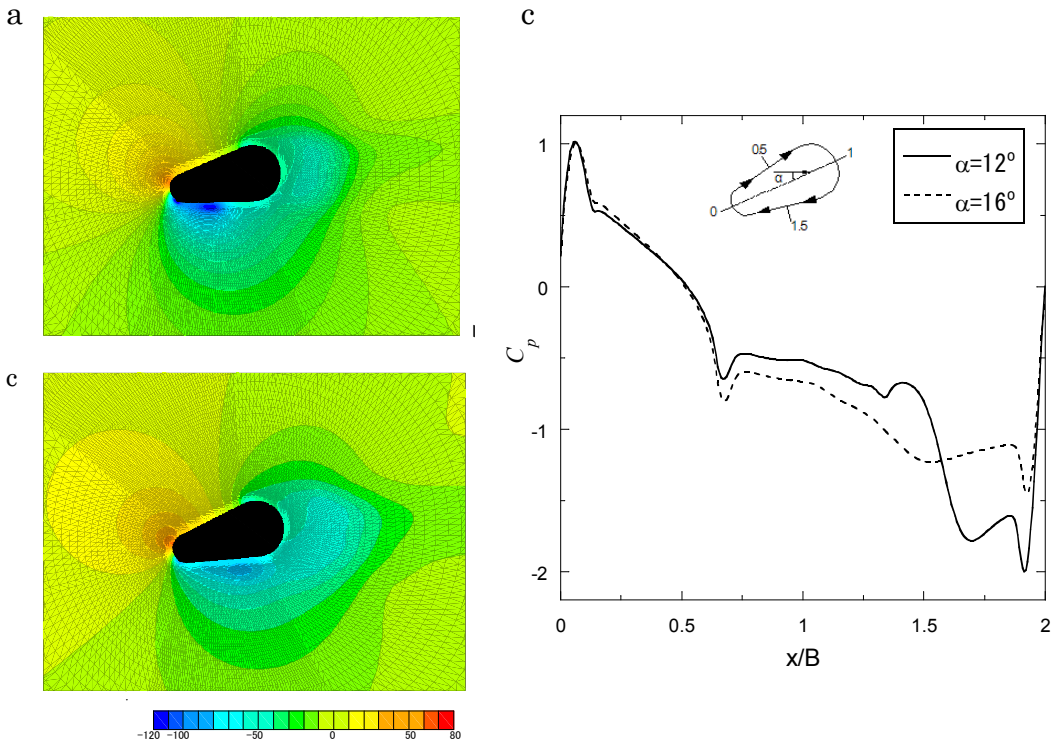

Figure 5. Mean pressure field : (a) $\alpha = 12°$; (b) $\alpha = 16°$; (c) mean surface pressure coefficients distributions

Figure 5 shows mean pressure field and mean surface pressure coefficients distributions in the vicinity of ice accreted single conductor at $\alpha = 12°$ and 16° for H=1*D*. As shown in Figure 5 (a) and (b), magnitude of negative pressure at around leading edge of lower face at $\alpha = 12°$ is larger than that at $\alpha = 16°$. This indicates that larger negative lift force is generated around $\alpha = 12°$, which resulted in the peak lift coefficient. As shown in Figure 5 (c), magnitude of negative pressure at around leading edge of lower face, x/B=1.6 to 1.9, is larger than that at $\alpha = 16°$. This indicates that larger negative lift force is generated at $\alpha = 12°$.

4 MEAN AERODYNAMICS FOR 4-CONDUCTOR BUNDLE

In this section, mean aerodynamic coefficients of 4-conductor bundle transmission line are estimated by the numerical simulation and by a proposed formula based on the predicted aerodynamic coefficients for the single conductor.

The predicted aerodynamic coefficients by the numerical simulation with angles of attack for 4-conductor bundle with H=1*D* are in good agreement with the experiment as shown in Figure 6. Aerodynamic coefficients of 4-conductor bundle can be described as follows;

$$C_{Da} = \frac{1}{2}(C_{D1} + C_{D2} + C_{D3} + C_{D4}) \tag{8}$$

where subscript a denotes 4-conductor bundle, and subscript 1 to 4 denote each conductor for 4-conductor bundle. Aerodynamic coefficients of each conductor maybe modified by using reduce factor, γ_i, from that of single conductor;

$$C_{Di} = C_D \times \gamma_i^2, \qquad \gamma_i = U_i / U_0 \tag{9}$$

where subscript i demotes each conductor. U_i and U_0 denote upstream wind velocity for each conductor and inflow velocity respectively.

Aerodynamic force coefficients in the wake region are proportional to velocity pressure. Suppose that distribution of velocity pressure in the wake region is in sinusoidal waveform where minimum and maximum velocity pressure are denoted as $1/2\rho U_{\min}^2$ and $1/2\rho U_{\max}^2$ respectively. Mean velocity pressure in the wake region can be estimated as follows:

$$1/2\rho U^2 = 1/2 \cdot \rho(U_{\min}^2 + U_{\max}^2)/2 \tag{10}$$

Normalized mean velocity pressure by the velocity pressure in the inflow, $1/2\rho U_o^2$ can be expressed as:

$$\gamma^2 = (\gamma_{\min}^2 + \gamma_{\max}^2)/2 \tag{11}$$

Figure 7 shows predicted non-dimensional mean velocity profile in y direction, normal to inflow direction in the upstream side of a rear conductor. Minimum reduce ratio is estimated 0.21 at $\alpha = 90°$ and maximum one is 0.86 resulting in $\gamma = 0.623$. Similarly, $\gamma = 0.867$ is obtained at $\alpha = 0°$. Table 3 shows mean drag coefficient of 4-conductor bundle from the experiment and the formula. Drag coefficients by present formula are closer to experiment, comparing with those obtained by conventional one.

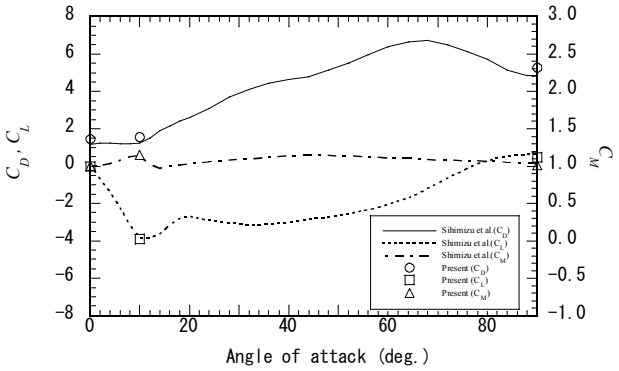

Figure 6. Variation of aerodynamic coefficients with angles of attack for 4-conductor bundle with H=1*D*

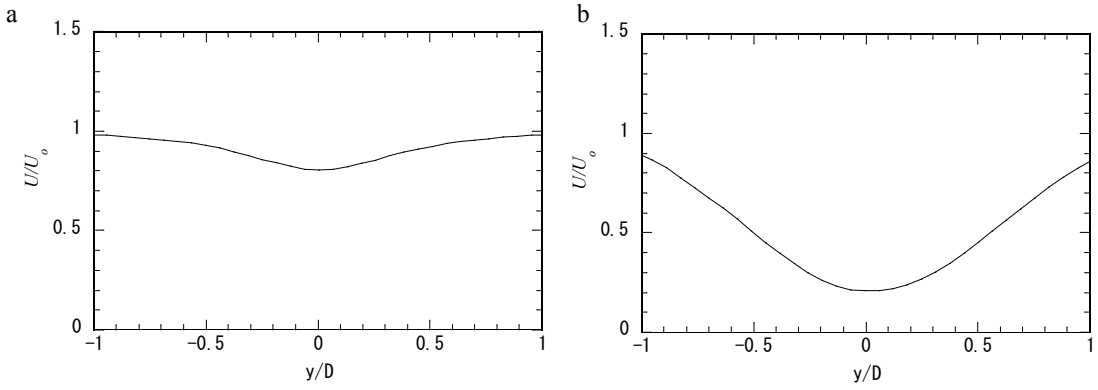

Figure 7. Non-dimensional mean velocity profile in y direction in the upstream side of a rear conductor: (a) $\alpha = 0°$; (b) $\alpha = 90°$.

Table 3. Mean aerodynamic coefficient of 4-conductor bundle

α	Experiment	Conventional	Present
0°	1.18	1.40	1.23
90°	4.84	6.94	4.83

5 CONCLUSION

Aerodynamic coefficients of ice accreted single and 4-conductor transmission line have been investigated using LES turbulence model. Following summarizes the findings and conclusions of this study;

1) The predicted mean aerodynamic coefficients of ice accreted single conductor with curved surfaces by the numerical simulation show good agreement with experiments, while lift coefficients obtained by interpolations significantly overestimated the experiments in some angle of attack.
2) It was found that peak negative lift coefficient for H=1*D* case is caused by negative pressures near the tip of the lower face. Negative pressures increase with increase in angle of attack and recovers at angle larger than 12° due to the vortex shedding. Intensive and concentrated negative pressure region was observed at $\alpha = 12°$, according to the peak lift coefficient at around this angle of attack.
3) A formula was proposed to estimate aerodynamic coefficients of 4-conductor bundle from corresponding those of single conductor, considering velocity reduction in the wake region. The predicted drag coefficients at $\alpha = 0°$ and 90° for 4-conductor agree well with the experiment and overestimations by the conventional formula are improved.

6 REFERENCES

Cooper, K. R., 1973. Wind tunnel and theoretical investigation into the aerodynamic stability of smooth and stranded twin bundled power conductors, National aeronautical establishment, Report LTR-LA-115.

Den Hartog, J. P., 1956. Mechanical vibrations, McGraw-Hill.

Ferziger, J., Peric, M, 2002. Computational method for fluid dynamics, 3rd Edition, Springer.

Inoue, M., 2000. Formulation of unsteady aerodynamic forces on an ice-accreted 4-conductor bundle transmission line and prediction of the wind-induced response amplitude.

Kimura, K., Inoue,M., Fjujino, Y., Yukino, T., Inoue, H., Morishima, H., 1999. Unsteady forces on an ice-accreted four conductor bundle transmission line, 467-472, ISMB 905809 059 0.

Novak, M., 1972. Galloping Oscillations of Prismatic Structure, Proc. ASCE, Vol. 98, No. EM1.

Oka, S., Ishihara, T., 2009. Numerical study of aerodynamic characteristics of a square prism in a uniform flow, Journal of Wind Engineering and Industrial Aerodynamics 97, 548-559.

Parkinson ,G. V., 1971. Wind-induced instability of structure, Phil. Trans. Roy. Soc. Lund. A 269, 395-409.

Phuc, P.V., Ishihara, T., Shimizu, M., 2005. A wind tunnel study on unsteady forces of ice accreted transmission lines, 5th International colloquium on bluff body aerodynamics and applications, 374-376. Ottawa.

Shimizu, M., Sato, J., 2001, Galloping observations and simulation of a -4condictor bundle transmission line, Jour nil of Structural Engineering, Vol. 47A,479-488.

Shimizu, M., Ishihara, T., Phuc, P. V., 2004. A Wind tunnel study of aerodynamic characteristics of ice accreted transmission lines, 5th International colloquium on bluff body aerodynamics and applications, 369-372. Ottawa.

Smagorinsky, J., 1963. General circulation experiments with the primitive equations. I. The basic experiment, Month. Wea. Rev. 91, 99-164.